Prss37 Is Required for Male Fertility in the Mouse 1

Authors: Shen, Chunling, Kuang, Ying, Liu, Jianbing, Feng, Jingsheng, Chen, Xiaoyi, et al.

Prss37 Is Required for Male Fertility in the Mouse[1]

Chunling Shen,[4,5] Ying Kuang,[3,6] Jianbing Liu,[7] Jingsheng Feng,[8] Xiaoyi Chen,[7] Wenting Wu,[6] Jun Chi,[6] Lingyun Tang,[7] Yifei Wang,[8] Jian Fei,[6] and Zhugang Wang[2,4,6,7]

[4]State Key Laboratory of Medical Genomics, Institute of Health Sciences, Shanghai Institutes for Biological Sciences, Chinese Academy of Sciences and School of Medicine, Shanghai Jiao Tong University, Shanghai, China
[5]Graduate School, Chinese Academy of Sciences, Shanghai, China
[6]Shanghai Research Center for Model Organisms, Shanghai, China
[7]Research Center for Experimental Medicine, Rui-Jin Hospital and Department of Medical Genetics, School of Medicine, Shanghai Jiao Tong University, Shanghai, China
[8]Department of Histology and Embryology, School of Medicine, Shanghai Jiao Tong University, Shanghai, China

ABSTRACT

In order to understand the mechanisms of mammalian fertilization, studies using genetically manipulated animals have provided us with plenty of interesting and valuable information on the genetic factors affecting male fertility. In the present work, we demonstrate for the first time that Prss37, a previously uncharacterized putative trypsin-like serine protease, is required for male fertility. Prss37 is highly and exclusively expressed in the testis of adult mice, especially in the elongating spermatids during spermiogenesis, and almost vanishes in the mature sperm of mice. Mice deficient for *Prss37* show male infertility, but their mating activity, spermatogenesis, sperm morphology, and motility remain unaffected. In vivo fertilization assays revealed that *Prss37*$^{-/-}$ mice exhibited a markedly decreased fertilization rate (2.3% vs. 70% of that in control mice) accompanied by the defect in sperm migration from uterus into oviduct. In vitro study further showed sperm were incapable of sperm-egg recognition/binding when zona-intact eggs were exposed to *Prss37*$^{-/-}$ sperm, in which mature Adam3 was completely undetectable. Interestingly, however, *Prss37*$^{-/-}$ sperm were able to fertilize cumulus-intact oocytes in vitro. These data clearly indicate that *Prss37* deficiency causes the absence of mature Adam3 in sperm and a defect in sperm migration from uterus into oviduct, which mainly accounts for male infertility of *Prss37*-null mice, while the defect in sperm-zona binding seems irrelevant to the fertilizing ability of *Prss37*$^{-/-}$ sperm.

gene expression, male infertility, sperm motility and transport, sperm-zona binding, transgenic/knockout model

INTRODUCTION

Male infertility can be caused by many different aspects, such as genetic, biological, and sexual problems. Clinical assessment of male fertility is usually based on semen analysis, including sperm count, sperm morphology, and motility [1]. However, unexplained male infertility occurs even with all normal semen parameters, in clinical practice [2]. In order to fertilize an egg, sperm are first produced through spermatogenesis, which includes three phases: mitosis, meiosis, and spermiogenesis [3]. Spermiogenesis is a highly regulated process, which involves dramatic morphological changes, such as transforming round spermatids into elongated, tadpole-like spermatozoa; forming acrosome and sperm tail; packing chromosomes, rearranging mitochondria, and surface transmembrane structures; and removing the cytoplasm residual body [3, 4]. Many spermatid-specific genes are expressed specifically during spermiogenesis to regulate and execute this reconstruction process [5–8]. Following spermiogenesis, spermatozoa are released from the apex of the seminiferous epithelium into the tubular lumen and undergo maturation during epididymal transit [9, 10]. Finally, ejaculated sperm must capacitate in the female genital tract and migrate into an oviduct before they reach, recognize, and fuse with the oocytes [11, 12].

The serine protease 37 precursor (Prss37), also known as Tryx2 and 1700016G05Rik, is a putative trypsin-like serine protease. Serine proteases, which have a nucleophilic Ser residue at the active site, account for approximately one-third of all known proteinases [13, 14]. It has been shown that sperm serine proteases are indispensible in the fertilization process like sperm capacitation and sperm–egg binding. Sperm from mice deficient for *Pcsk4*, a serine protease, display accelerated capacitation, precocious acrosome reaction (AR), reduced binding to egg zona pellucida (ZP), and impaired fertilizing ability [15, 16]. Also, mice lacking two other serine protease genes, acrosin (*Acr*) and *Prss21*, show male subfertility [17]. Although single-knockout *Acr* or *Prss21* males are fully fertile, *Acr*$^{-/-}$ mouse sperm show altered rates of protein dispersal from the acrosome and delayed penetration of the ZP, and *Prss21*$^{-/-}$ mouse sperm exhibit reduced ability to bind the ZP and undergo ZP-induced AR, as well as the severely impaired ability to fuse with the egg in vitro [18–20]. Prss37 may play a role similar to that of the above-mentioned serine proteases, even though its enzyme activity has not been demonstrated. Mouse *Prss37*, located on chromosome 6B2 and composed of six exons, encodes a 237-amino acid (aa) protein. Human *PRSS37* is located on chromosome 7q34 and is composed of

---

five exons spanning 5144 bp. Two isoforms for human *PRSS37* have been identified, with one encoding a 235-aa protein and the other encoding a 234-aa protein because of an alternative splicing event at the end of exon 3. Protein sequence analysis reveals that Prss37 is highly conserved among various species, suggesting an important evolutionarily conserved role for this protein. However, the physiological function of Prss37 remains unknown.

In this study, we investigate the expression pattern of Prss37, describe a targeted mutation of *Prss37* in the mouse, and show that Prss37 is expressed exclusively in the spermatids at steps 9–14 of spermiogenesis and is required for male fertility in the mouse. The underlying causes of reproductive defects in male mice are analyzed and discussed.

MATERIALS AND METHODS

Ethics Statement

All research protocols involving animal experiments were approved by Institutional Animal Care and Use Committee of Shanghai Research Center for Model Organisms.

mRNA Expression Analyses

The relative expression levels of *Prss37* in the indicated mouse tissues were assayed by both reverse-transcription (RT)-PCR and real-time PCR. Total RNA was isolated using Trizol reagent (Invitrogen). A 2-μg sample of total RNA was reverse transcribed using Moloney murine leukemia virus reverse transcriptase (Promega). cDNA was amplified using specific sets of primers. Primer sequences for *Actb* and *Prss37* in the RT-PCR assays were 5′-GCCTTCCTTCTTGGGTATG-3′ (forward) and 5′-ACGCAGCTCAG TAACAGTCC-3′ (reverse) for *Actb*; and 5′-AATCCCTGCGTGGGTGTC -3′ (forward) and 5′-GGCTGCTTCCTTGTTGAGT-3′ (reverse) for *Prss37*. Amplification products were separated by electrophoresis on 1.0% agarose gels and visualized by ethidium bromide staining. Real-time PCR was performed with a Mastercycler ep realplex (Eppendorf) using the double-stranded DNA-specific fluorophore SYBR Green (catalog number DRR081A; TaKaRa, Japan). The primer sequences for *Actb* and *Prss37* in real-time PCR assay were 5′-TACCCAGGCATTGCTGACAGG-3′ (forward) and 5′-ACTTGCGGTGCACGATGGA-3′ (reverse) for *Actb*; and 5′-CCTGCCACCTTCAACCACAA-3′ (forward) and 5′-GGCTGC TTCCTTGTTGAGT-3′ (reverse) for *Prss37*. Resolution of the product of interest from nonspecific product amplification was achieved by melting curve analysis. Expression level of *Prss37* was normalized to *Actb* content.

Western Blotting

Testes, epididymides, and mature sperm collected from the cauda epididymides of mice were lysed in DIGE lysis buffer (7 M urea, 2 M thiourea, 4% 3-[(3-cholamidopropyl)dimethylammonio]-1-propanesulfonate (CHAPS), 30 mM Tris, pH 8.5). After centrifugation at 12 000 rpm for 30 min, the supernatant was harvested, and protein concentration was determined using the Bradford method. Samples were supplemented 6-fold concentrated SDS-PAGE sample buffer containing 2-mercaptoethanol and boiled at 100℃ for 5 min. Equal amounts of proteins (60–80 μg) were separated by 10% SDS-PAGE and transferred to nitrocellulose membranes (catalog no. 162-0112; Bio-Rad). Membranes were blocked with 5% nonfat milk for 1 h, followed by incubation with the primary antibodies as indicated overnight at 4℃. Antibodies used were a rabbit polyclonal antibody raised against Prss37 (1:1000 dilution; code HPA020541; Sigma-Aldrich), a mouse monoclonal antibody against Gapdh (1:1000 dilution; code M20006; Abmart), a mouse monoclonal antibody against Actb (1:1000 dilution; code sc-47778; Santa Cruz Biotechnology), a mouse monoclonal antibody against Adam3 (1:1000 dilution; code MAB19291; Millipore), a mouse monoclonal antibody against Adam2 (1:1000 dilution; code MAB19292; Millipore), a rabbit polyclonal antibody against Adam1 (1:1000 dilution; code ab65876; Abcam), a rabbit polyclonal antibody against Pdilt (1:1000 dilution; code ab116182; Abcam), a mouse monoclonal antibody against Calr3 (1:1000 dilution; code WH0125972M1; Sigma), a rabbit polyclonal antibody against Matn1 (1:1000 dilution; code SAB3500034; Sigma), and a rabbit polyclonal antibody against Atp5a1 (1:1000 dilution; code 14676-1-AP; Proteintech). The secondary antibodies conjugated with IRDye 800CW (Li-Cor) were used to visualize the specific protein bands by using an infrared imager (the Odyssey; Li-Cor).

Gapdh, Actb, or irrelevant sperm proteins (Matn1 and Atp5a1) were used as loading controls.

Immunohistochemistry

Testes and epididymides were fixed in Bouin buffer (combined 75 ml of saturated picric acid, 25 ml of formalin, and 5 ml of glacial acetic acid) and embedded in paraffin. Tissue sections were blocked in 5% normal goat serum in PBS at room temperature for 1 h and incubated overnight at 4℃ with diluted anti-Prss37 rabbit antiserum (1:100 dilution; Sigma). After three washes in PBS for 5 min each, sections were detected with an ABC kit (Vectastain; Vector Labs) according to the manufacturer's instructions.

Generation of Prss37 Targeting Vector

Prss37 targeting vector was achieved by ET cloning [21, 22]. Briefly, homology arms A, B, C, and D were amplified from a bacterial artificial chromosome (BAC) clone (bMQ-302A10; Source Bioscience) containing *Prss37* genomic sequence. Primers were 5′-AATAAGCTTTTTAGA-TAGCCCTGTCCT-3′ for A1 and 5′-TTCCTCGAG CATTTACTGCCTCTTTCAT-3′ for A2; 5′-CGCCTCGAGTGGCATAGAG CAGGAGAC-3′ for B1 and 5′-CGCGGTACCCAACATTGGACCA GAAGC-3′ for B2; 5′-AATCCGCGGTCAAGCGACAATTATGAAC-3′ for C1 and 5′-AATGGATCCTCCCAGCAGTAAAGAAGTA-3′ for C2; and 5′-ATAAAGCTTGGTGGGATGGAGTAGAAA-3′ for D1 and 5′-ATAGTC GACCACCTCCTTAATGTAAATGG-3′ for D2. PCR products A and B were digested by *Hind*III-*Xho*I and *Xho*I-*Kpn*I, respectively, and inserted into the *Hind*III-*Kpn*I sites of pBR322-MK-MCS containing a herpes simplex virus thymidine kinase (HSV-TK) negative selection cassette to produce the retrieving vector pBR322-MK-MCS-AB. After linearization by *Xho*I, genomic DNA containing *Prss37* was retrieved from the BAC by the obtained retrieving vector. Similarly, PCR products C and D were digested by *Sac*II-*Bam*HI and *Hind*III-*Sal*I, respectively, and ligated to the *Sac*II-*Bam*HI and *Hind*III-*Sal*I sites of PL451 vector containing the neomycin resistance gene (PGK-Neo). C-Neo-D fragment was amplified from the vector by using C1 and D2 primers and knocked into pBR322-MK-MCS-AB to obtain the targeting vector. The targeting vector contained homology arms of 4756 bp (5′) and 3543 bp (3′).

Generation of Prss37 Knockout Mice

The targeting construct was linearized with *Not*I and electroporated into SCR012 embryonic stem (ES) cells. Resistant cells were selected in the presence of G418 (G418 sulfate; Geneticin ; Gibco) and ganciclovir. DNA was isolated from a total of 128 clones and analyzed by PCR to identify positive clones that had undergone homologous recombination with the targeting vector. Primers for 5′ arm and 3′ arm evaluation were 5′-CGAG-CATCCTGGCTTATC-3′ for P1 and 5′-CCACTCCCACTGTCCTTT-3′ for P2; and 5′-TTTATTAGGAAAGGACAGTGGGAGT-3′ for P3 and 5′-TCTGTGAAGTAGGGATGGGTTGT-3′ for P4, with 5520-bp and 4459-bp product lengths, respectively. Two independent ES cell clones were injected into C57BL/6J blastocysts, which were subsequently transferred into pseudopregnant females to generate chimeric offspring. Chimeras were bred with C57BL/6J female mice to produce heterozygotes. All mice were housed in a temperature-controlled facility in rooms maintained at a 12L:12D cycle, with free access to a diet of regular chow and water.

Genotyping of Mutant Mice

The genotypes of mutant mice were determined by PCR of genomic DNA extracted from mouse tails with specific primers for wild-type (wt) allele (P5, 5′-ACTAGTTATAGCTCTTGATGCC-3′; and P6, 5′-CGAGTTTTAGGT GAAGACATC-3′) and targeted allele (P5 and P7, 5′-TGTCATCT CACCTTGCTCCT-3′). The three primers were used in a multiplex PCR with ExTaq (Takara), with the following amplification conditions: 95℃ for 4 min and 35 cycles of 94℃ for 30 sec, 62℃ for 30 sec, 72℃ for 1 min 20 sec, and a 10-min incubation at 72℃ at the end of the run. PCR products were resolved on 1.0% agarose gels. Product lengths of wt and targeted alleles were 642 bp and 1138 bp, respectively.

Reproductive Capacity Evaluation

Adult male mice of three genotypes (n ≥ 5 males each group) were caged with wt females at a male-to-female sex ratio of 1:2, respectively. Any plugged female was removed and replaced. Male mice were given two new females every week. This regimen lasted for 30 days. Plugged mice that gave birth to

offspring were recognized as pregnant. The number of total females, plugged females, litters, and offspring were counted to calculate frequency of copulatory plug (FCP) and frequency of conception (FC).

Histological Analysis

Testes from adult age-matched mice with different genotypes were isolated and weighed. Testes and cauda epididymides were fixed and embedded in paraffin as described above. Tissue sections were stained with hematoxylin and eosin (H&E) according to standard protocols. Sperm were isolated from cauda epididymides of wt and *Prss37*$^{-/-}$ mice and spotted onto glass slides and stained with H&E.

Transmission Electronic Microscopy

Transmission electron microscopy (TEM) was performed at the Laboratory of Electron Microscopy, Shanghai Jiaotong University School of Medicine, following standard protocols [23]. Briefly, sperm were isolated from cauda epididymides of both wt and *Prss37*$^{-/-}$ mice, fixed in glutaraldehyde and osmic acid, infused in 10% gelatin, dehydrated in sucrose, and then frozen in liquid nitrogen. Cryosections (50 nm) were prepared using a cryo-ultramicrotome (Ultra-Cut UCT/Leica EMFCS) and stained with uranyl acetate and methylcellulose and observed by TEM.

Computer-Assisted Semen Analysis

Parameters of sperm motility were quantified by computer-assisted semen analysis (CASA) using integrated visual optical system software (Hamilton-Thorne Biosciences). Briefly, one side of the cauda epididymidis was dissected from each mouse (2–3 months old) and put into a 1.5-ml Eppendorf tube containing 500 μl of human tube fluid (HTF) medium [24] at 37°C. Cauda epididymides were cut to allow sperm to get out. After a 5-min incubation, capacitated sperm from the upper layer of the medium were added to a counting chamber for analysis. More than 1000 sperm were examined for each sample.

Induction of Acrosome Reaction

Sperm from cauda epididymides were incubated in HTF medium at 37°C in a humidified incubator with 5% CO_2 in air to allow capacitation. After 1 h, a part of the capacitated sperm was spotted onto glass slides, and the other part of the capacitated sperm was added to a calcium ionophore (A23187; Sigma), at a final concentration of 10 μmol/L to induce AR. After an additional 30-min incubation, sperm were spotted onto glass slides and air dried. Acrosome status was evaluated by staining with Alexa Fluor 647-conjugated lectin peanut agglutinin (PNA; Molecular Probes), which binds to the outer acrosomal membrane and therefore, does not stain acrosome-reacted sperm [25, 26].

Activity of Acrosomal Enzymes

Cauda epididymal sperm were capacitated in 500 μl of HTF at 37°C under 5% CO_2 in air for 1 h. Sperm mixtures were counted using a hemocytometer. Different amounts of sperm (1×10^6, 2×10^6, 4×10^6) were divided into 1.5-ml Eppendorf tubes and centrifuged at $2000 \times g$ for 10 min. The activity of acrosomal enzymes was measured using *t*-butyloxycarbonyl (Boc)-Phe-Ser-Arg-4-methylcoumaryl-7-amide (MCA) as substrate. The reaction mixture (0.5 ml) consisted of 50 mM Tris-HCl (pH 8.0), 10 μM substrate, and an appropriate amount of acrosomal enzymes. Following incubation at 37°C for 20 min, the amount of 7-amino-4-methylcoumarin released was fluorometrically determined with excitation at 380 nm and emission at 460 nm (BioTek Synergy 2; Gene Company Limited).

In Vivo Fertilization Assay

wt female mice were superovulated by intraperitoneal injection of 5 units of pregnant mare serum gonadotropin, followed by 5 units of human chorionic gonadotropin (hCG) 46–48 h later, and were mated with wt and mutant male mice. The oviducts were excised from the mice which formed copulation plugs 27 h and 45 h after hCG injection. Pronuclear-stage or two-cell embryos were recovered from the oviducts. Pronuclear-stage embryos were stained with Hoechst 33258 dye and observed under fluorescence microscopy. Two-cell embryos were counted under light microscopy, and fertilization rate was calculated as the ratio between the number of two-cell embryos recovered and the total number of two-cell embryos plus oocytes recovered.

Sperm Count in Oviducts

Superovulated wt female mice were caged together with test males for 0.5 h after hCG injection. The formation of vaginal plugs was checked every hour. Oviducts (two sides) of plugged females were excised 3.5 h after coitus, and sperm inside the oviducts were flushed out with 1 ml of M2 medium (Sigma) into a culture dish (3037; Falcon). Sperm in the center circle were counted and analyzed.

Sperm Migration Analysis

Superovulated wt female mice were caged with test males for a 2-h mating time (9–11 h after hCG injection) [27] and checked for the formation of vaginal plugs. Uteri and oviducts of plugged females mated with wt or *Prss37*$^{-/-}$ males were excised and fixed 2 h after coitus [28, 29], and paraffin-embedded serial sections were made and stained with H&E. Sperm transits from uterus into oviducts were analyzed by observation of sections containing utero-tubal junction (UTJ).

Sperm-Egg Binding Assay

wt eggs were collected and freed from cumulus cells with 0.01% (w/v) hyaluronidase (H-3757; Sigma). Half of the cumulus-free eggs were treated with acidic Tyrode solution (Sigma) for approximately 30 sec to remove the ZP. The zona-intact and zona-free eggs were co-incubated with the cauda epididymal sperm (10^5–10^6 sperm) collected from wt or mutant mice and capacitated in vitro for 1 h in HTF medium. After 15 min of co-incubation, the eggs were washed gently with HTF medium, and sperm bound to ZP or egg plasma membrane were observed.

In Vitro Fertilization Assay

The oocyte-cumulus complexes (OCCs) were isolated from superovulated female mice 14 h after hCG injection. The OCCs in HTF medium were mixed with capacitated epididymal sperm and incubated at 37°C under 5% CO_2 in air. After 6 h, eggs were washed and transferred to potassium simplex optimized medium [30] for culture to later stages.

Statistical Analysis

All data are mean values $\pm$ SEM ($n \geq 3$), unless otherwise stated. The Student *t*-test was used for statistical analysis; significance was assumed for a *P* value of <0.05.

RESULTS

Testis-Exclusive and Stage-Specific Expression Pattern of Prss37 in Adult Mice

The relative expression levels of *Prss37* in mouse tissues were assayed in cDNA samples prepared from 16 mouse tissues including cerebrum, cerebellum, thymus, heart, lung, liver, spleen, kidney, stomach, intestine, bladder, skeletal muscle, testis, epididymidis, ovary, and uterus. Both the RT-PCR and real-time PCR assays detected a unique transcript of mouse *Prss37* exclusively and dominantly in testis tissue (Fig. 1A). Because testis maturation is age-dependent, the first wave of spermatogenesis takes place within 35 postnatal days [31]. In order to determine the temporal and spatial expression of *Prss37* in testis, we examined the *Prss37* mRNA abundance in testis and epididymidis of mice at 7, 14, 18, 21, 23, 28, and 42 postnatal days by using real-time PCR. Results showed that *Prss37* mRNA first appeared at approximately 23 postnatal days in the testis, and no *Prss37* mRNA could be detected in the epididymidis (Fig. 1B). Moreover, Western blot analysis of testis and epididymidis lysates from 2-, 4-, 6-, and 8-week-old mice showed that Prss37 protein existed solely in the testis but not in epididymidis (Fig. 1C). The first appearance of Prss37 protein in the testis was determined on postnatal day 28 by narrowing down the time range examined (Fig. 1D). Thus, there was a time gap of approximately 5 days between *Prss37* expression and translation. The time gap between gene transcription and translation has been reported by others as well [4, 32, 33]. Further histoimmunochemistry analyses of
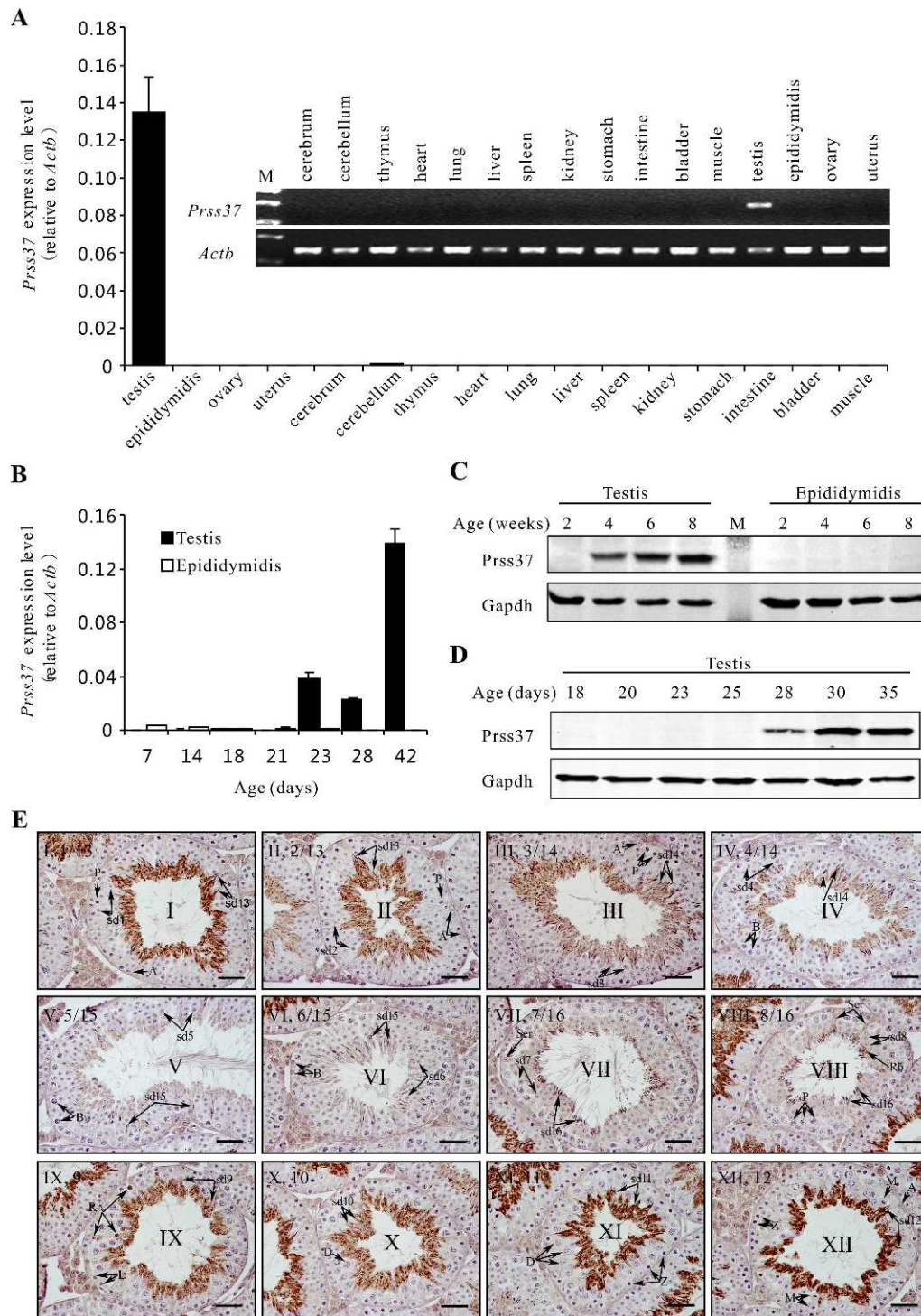
3

Article 123

FIG. 1. *Prss37* gene expression profile. **A**) Tissue-specific expression of *Prss37* mRNA as revealed by both RT and real-time PCR. Total RNAs isolated from the indicated tissues were reverse transcribed with MMLV-RT, and the cDNA templates were then used to amplify a specific region of the *Prss37* coding sequence (see *Materials and Methods*). Bar chart shows mean ± SEM values from five replicates relative to *Actb* mRNA levels. The agarose gel electrophoresis images represent RT-PCR. *Actb* was used as a loading control. M, DNA markers. **B**) *Prss37* mRNA expression in testis and epididymidis by real-time PCR during the early development of male mice. Each cDNA sample was a mixture derived from 2–3 mice. Values are means ± SEM from three replicates relative to *Actb* mRNA levels. **C**) Western blot analysis of Prss37 in testis and epididymidis from the mice of indicated ages. Gapdh was used as a loading control. Lane M, protein molecular weight markers. **D**) Prss37 protein first appeared at approximately 28 postnatal days, corresponding to the elongating stage of spermiogenesis. **E**) Immunohistochemical localization of Prss37 protein in the adult mouse testis. Each image exhibits a stage of the seminiferous epithelial cycle and the corresponding steps of spermatid development, denoted by Roman numerals and Arabic numbers, respectively, at the top left corner of each image. A, type A spermatogonia; B, type B spermatogonia; D, diplotene; L, leptotene; P, pachytene; Rb, residual body; sd, spermatid; Ser, sertoli cell; Z, zygotene. Prss37 was restrictively expressed at stages I–IV and IX–XII of the seminiferous epithelial cycle, corresponding to the spermatids at steps 9–14 of spermiogenesis. Bar = 25 μm.
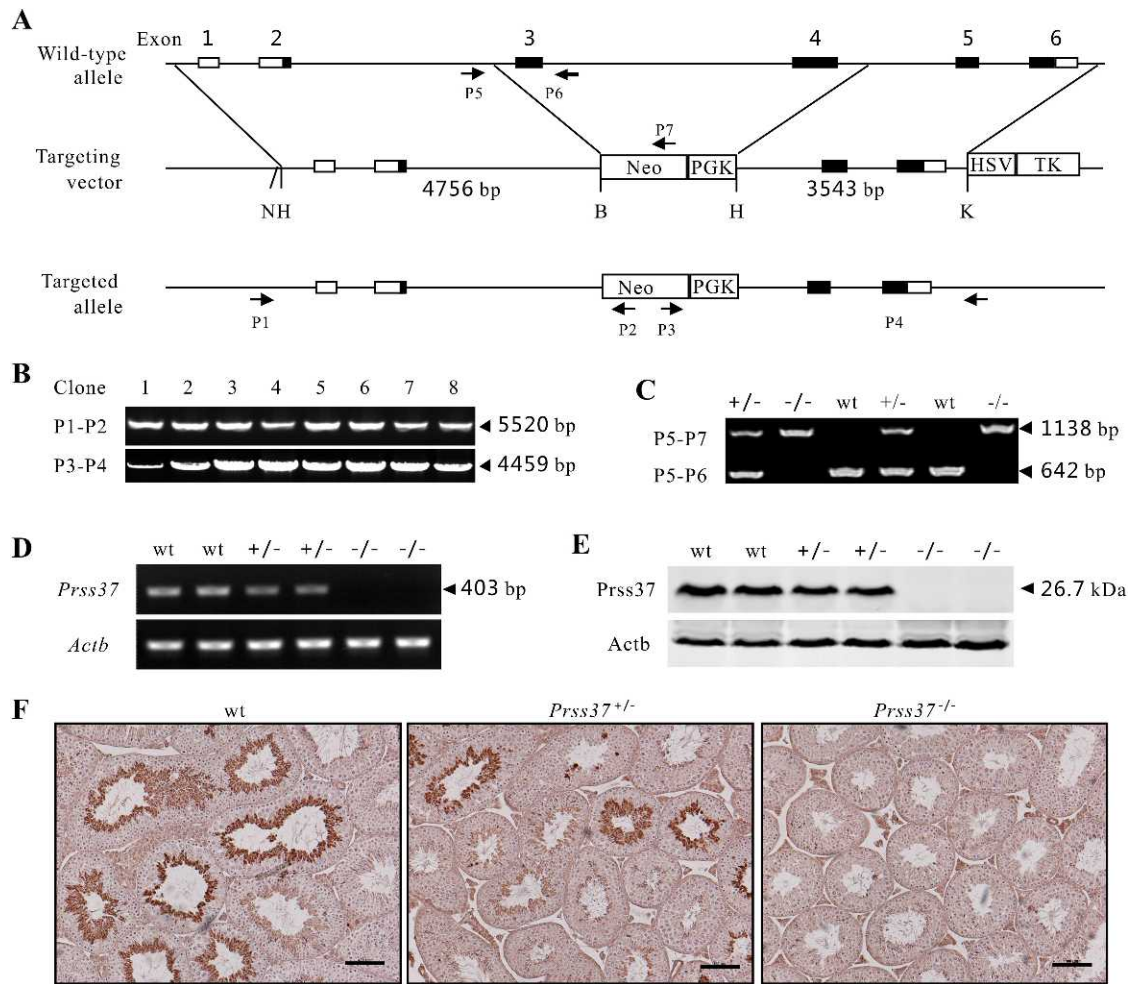
FIG. 2. Targeted disruption of *Prss37* gene. **A**) Complete structures of the wt mouse *Prss37* allele. Exons and introns are represented by boxes and horizontal lines, respectively. The coding region is shown in black. For the targeted disruption of mouse *Prss37* allele, the targeting vector contained 4756 bp of 5′ homology and 3543 bp of 3′ homology. Homologous recombination resulted in the replacement of exons 3 and 4 by Neo. HSV-TK was introduced into the targeting vector for negative control. P1–P7, primers for genotyping; N, *Not*I; H, *Hind*III; B, *Bam*HI; K, *Kpn*I. **B**, **C**) Genotyping of positive ES cell clones and mouse tail tip DNA by PCR amplification with primers indicated on the left of the images. The relative sites of the primers are shown in **A**. The size of PCR products (arrowhead) is indicated on the right of the images. **D**) RT-PCR with total testicular RNA and primers amplifying a specific region of the *Prss37* coding sequence. A 403-bp fragment was obtained only in wt and heterozygous (+/–) animals. *Actb* was used as an internal control. **E**, **F**) Western blot and immunohistochemistry analyses of testis tissues from wt, +/– and homozygous (–/–) mice. Actb was used as a loading control in the Western blot. The molecular mass position of Prss37 is shown. **F**) Bar = 100 μm.

sections of adult mouse testis revealed that Prss37 was restrictively expressed at stages I–IV and IX–XII of the seminiferous epithelial cycle, corresponding to the spermatids at steps 9–14 of spermiogenesis [34] (Fig. 1E). We could exclude the expression of Prss37 in steps 1–4 of spermiogenesis by two points listed below: first, the paraffin-embedded sections were made from 8- to 12-week-old mice, so steps 1–4 overlapped with steps 13 and 14; second, steps 1–4 of spermiogenesis took place much earlier than postnatal day 28, when Prss37 protein was first detected. Taken together, Prss37 is exclusively expressed in the testis, especially at steps 9–14 of spermiogenesis. Such a specific expression pattern might indicate an important physiological role of Prss37 during spermiogenesis in mice.

Generation of Prss37-Deficient Mice

The translated region of the mouse *Prss37* gene includes six exons spanning approximately 4.7 kb on mouse chromosome 6B2. To determine the function of *Prss37* in vivo, we constructed a targeting vector using ET cloning method and used homologous recombination in ES cells to disrupt the *Prss37* gene. Exon 3 and exon 4 were replaced by PGK-Neo (Fig. 2A). Eight ES cell clones were identified positive by PCR using primers P1 and P2 to the 5′ arm and P3 and P4 to the 3′ arm (Fig. 2B). Two independent ES cell clones were injected into blastocysts to generate chimeras. Male chimeras were crossed with C57BL/6J females to establish strains with a mixed genetic background (129-C57) heterozygous for the mutated allele. Homologous recombination in offspring was confirmed in DNA (Fig. 2C), mRNA (Fig. 2D), and protein levels (Fig. 2, E and F). Therefore, we generated *Prss37*-null mice with a complete inactivation of the *Prss37* gene.

Prss37$^{-/-}$ Males Are Infertile and Have Normal Spermatogenesis, Sperm Morphology and Motility, and Comparably A23187-Induced AR and Activity of Acrosomal Enzymes

Intercrossing of heterozygous mice produced the offspring following Mendelian inheritance and showing grossly normal

TABLE 1. Targeted disruption of *Prss37* leads to male infertility in mice.

Male mice	Females	Plugs	Litters	Offspring (M/F)*	FCP (%)†	FC (%)‡
wt (n = 5)	79	29	24	145 (79/66)	36.7	82.8
Prss37+/− (n = 5)	82	32	19	137 (80/57)	39.0	59.4
Prss37−/− (n = 12)	182	62	0	0	34.1	0

* M, male; F, female.
† Frequency of copulatory plug (FCP) was calculated as the ratio of the number of plugged females to total number of females to which males with the same genotype had accessed.
‡ Frequency of conception (FC) was calculated as the ratio of the number of females that gave birth to offspring to the number of females with successful mating.

development. The prominent and testis-restricted expression of *Prss37* impelled us to investigate the reproductive phenotype of the *Prss37*−/− male mice. In the present study, each male mouse with different *Prss37* genotypes was allowed to continuously mate with wt females at a 1:2 male-to-female sex ratio. No differences were observed in the ability of male mice of any genotype to plug wt females, but no plugged females mated with *Prss37*−/− males became pregnant, suggesting that Prss37 protein is indispensible in male fertility (Table 1). On the other hand, *Prss37*−/− females were fertile when they were mated with wt or *Prss37*+/− males. All six *Prss37*−/− females mated with three wt and three *Prss37*+/−

males delivered pups during 2 months, which was consistent with the testis-exclusive expression pattern of *Prss37* in adult mice, with no expression of *Prss37* in ovary and uterus (Fig. 1A).

To elucidate the underlying mechanisms which led to the infertility of *Prss37*−/− males, we paid close attention to the development and phenotypes of *Prss37*−/− males. On reaching sexual maturity, wt, *Prss37*+/−, and *Prss37*−/− littermates were similar with regard to body and testis weight (Fig. 3A). There were no differences in gross morphology and histology of testis, cauda epididymidis, and sperm as indicated by H&E staining and light microscopy analysis (Fig. 3, B and C).
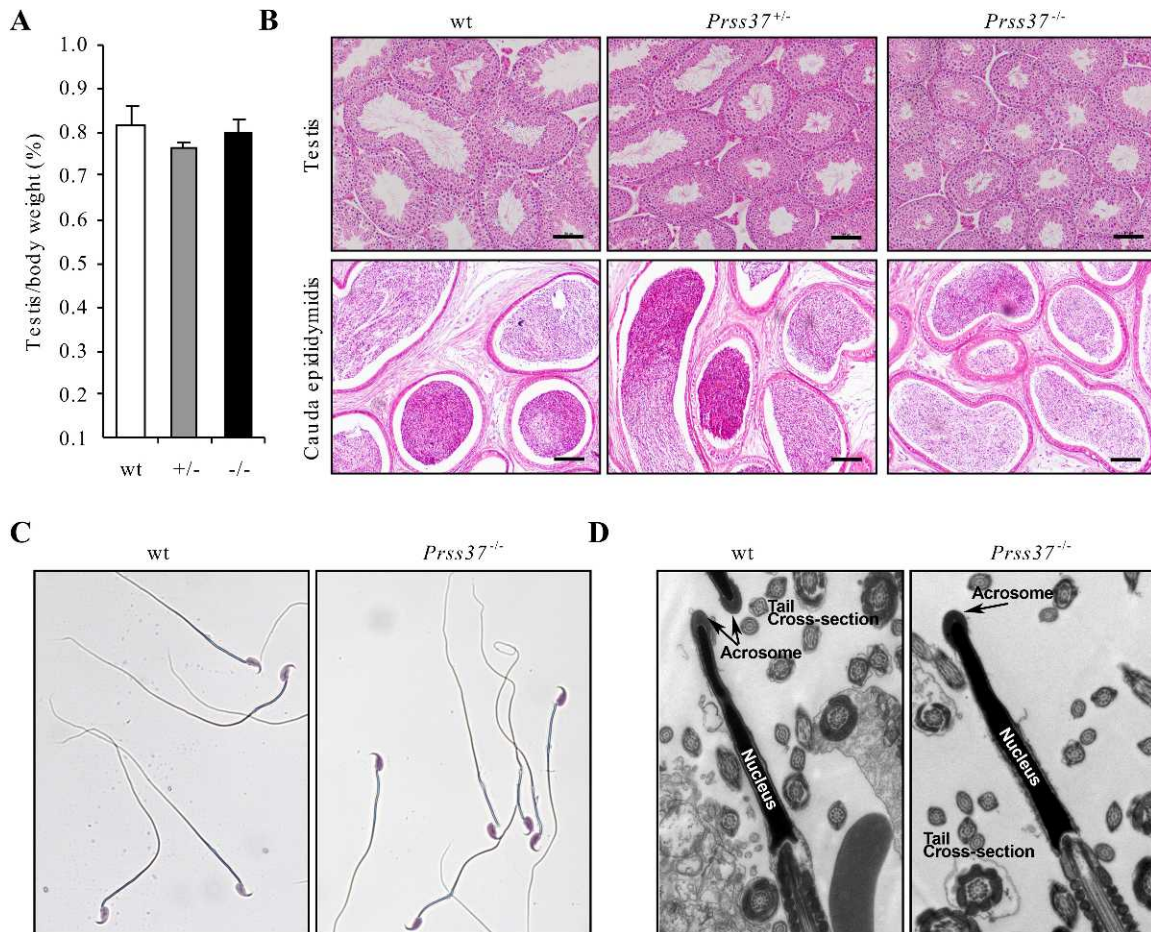

FIG. 3. Morphological and histological analyses of testis, cauda epididymidis, and sperm from mice of different genotypes. **A**) Testis size of mice of three genotypes was assessed by the ratio of testis weight to body weight (n = 5 for wt and −/−; n = 3 for +/−). **B**) H&E-stained sections of testis and cauda epididymidis from mice of three genotypes. All showed robust spermatogenesis. Bar = 100 μm. **C**) H&E-stained sperm smear preparations. Sperm were isolated from cauda epididymides of wt and *Prss37*−/− mice and spotted onto glass slides. No obvious sperm abnormalities were observed under light microscopic analysis. **D**) TEM images of sperm ultrastructures are shown. No obvious abnormalities of acrosome regions and tail cross-sections could be observed.

TABLE 2. Comparable motility of capacitated cauda epididymal sperm from wt and *Prss37*−/− males.*

CASA parameter	wt[†]	*Prss37*−/−[†]
Total motility (%)	93.2 ± 2.2	93.7 ± 1.3
Progressive motility (%)	58.5 ± 5.9	59.4 ± 2.2
Rapid motility (%)	66.9 ± 6.0	67.7 ± 2.5
Static cell (%)	6.8 ± 2.2	6.3 ± 1.3
Path velocity (μm/sec)	139.6 ± 5.6	147.3 ± 2.9
Prog. velocity (μm/sec)	109.2 ± 5.3	114.6 ± 2.8
Track speed (μm/sec)	243.5 ± 5.4	248.5 ± 4.1
Lateral amplitude (μm)	12.2 ± 0.3	13.0 ± 0.2
Beat frequency (Hz)	24.1 ± 0.6	23.0 ± 0.9
Straightness (%)	77.2 ± 0.9	77.2 ± 0.7
Linearity (%)	47.2 ± 1.2	48.2 ± 0.7
Elongation (%)	94.0 ± 1.1	94.4 ± 0.7

* Cauda epididymal sperm were capacitated by incubation in HTF medium and subjected to CASA. At least 1000 sperm were examined for each sperm sample (n = 5 for each genotype).
[†] Data in sperm analysis are means ± SEM. No significant differences in all parameters were found between wt and *Prss37*−/− sperm ($P > 0.05$).

Moreover, further investigation of the ultrastructures of *Prss37*−/− sperm by TEM suggested intact acrosome region and other ultrastructures of the sperm (Fig. 3D). All these observations suggested that sperm production and morphology were unlikely to be involved in the infertility of *Prss37*−/− males. Whether sperm motility activation after being released from cauda epididymidis would be affected due to *Prss37* deficiency remains unresolved. Again, there were no significant differences in the movement characteristics of capacitated sperm, as assessed by CASA. All parameters, including progressive motility, rapid motility, path velocity, and lateral amplitude, were comparable between wt and *Prss37*−/− sperm (Table 2).

Integrity of acrosome and timely occurrence of AR of the capacitated sperm were believed essential for sperm to fertilize an egg [35]. Therefore, we evaluated the percentage of acrosome-intact sperm in capacitated sperm from *Prss37*−/−

males and their response to the AR-inducer A23187. Thirty-minute incubation of sperm with A23187 induced more than 50% of sperm to undergo AR, comparable between wt and *Prss37*−/− sperm (Fig. 4A and Supplemental Fig. S1; all supplemental data are available online at www.biolreprod.org). Furthermore, the activity of acrosomal enzymes, as measured by Boc-Phe-Ser-Arg-MCA as substrate [36], showed no significant difference between wt and mutant sperm (Fig. 4B). In addition, *Prss37* disruption did not affect cumulus cell dispersal (Supplemental Fig. S2), unlike *Prss21* and *Acr*, double-knockouts of which significantly delayed the cumulus cell dispersal [17]. Thus, the AR or the activity of acrosomal enzymes could not be the cause of *Prss37*−/− male infertility.

Prss37−/− Males Show Severely Reduced In Vivo Fertilization Rate and Defect in Sperm Migration from Uterus into Oviducts

To further confirm the male infertility phenotype of *Prss37*−/− males, we recovered fertilized oocytes from the oviducts after natural mating between the wt females and wt or *Prss37*−/− males. The pronuclear and two-cell stage embryos (27 h and 45 h after hCG injection), which had been fertilized by the wt sperm, were retrieved at high level (approximately 70%, ratio between the number of embryos recovered and the total number of embryos plus oocytes recovered). In the case of *Prss37*−/− sperm, the percentages of these two kinds of embryos were significantly lower (approximately 2.3%) (Fig. 5, A and B), suggesting that the reproductive inability of *Prss37*−/− males could be caused by the incompleteness of fertilization.

For fertilization to occur in mammals, ejaculated sperm must migrate from uterus into oviducts and reach the egg. To address whether the reduced fertilization rate was due to impaired oviduct-migrating ability of the mutant sperm, sperm that had migrated into oviducts of plugged females 3.5 h after coitus with wt or *Prss37*−/− males were counted and analyzed. More than 300 wt sperm were recovered, while the number of
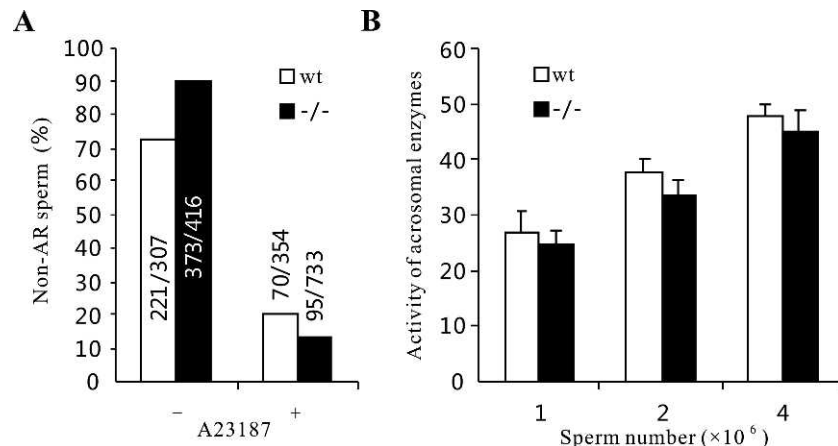

FIG. 4. Comparison of A23187-induced AR and the activity of acrosomal enzymes between wt and *Prss37*−/− sperm. **A**) Capacitated sperm before and after A23187 induction were counted, and percentages of non-acrosome-reacted (non-AR) sperm were analyzed. Sperm from the cauda epididymides were capacitated in vitro. Spontaneous and A23187-induced AR were examined by PNA staining after spotting sperm onto glass slides (see *Materials and Methods*). For each glass slide at least 10 different fields were examined. Representative images are shown in Supplemental Figure S1 (all Supplemental Data are available online at www.biolreprod.org). The total number of non-AR sperm (PNA positive [see Supplemental Fig. S1]) and the total number of sperm (DAPI-positive [see Supplemental Fig. S1]) analyzed in each group are indicated in the graph. This experiment was repeated three times, and values are data from a representative experiment. **B**) The activity of acrosomal enzymes of wt or *Prss37*−/− sperm was measured using Boc-Phe-Ser-Arg-MCA as substrate. The amount of sperm from one mouse ([0.8-1.4] $\times 10^7$ sperm/ml $\times$ 1 ml/mouse) was enough to be divided into three groups: 1×10^6, 2×10^6, and 4×10^6. For each group, three wt males and three *Prss37*−/− males were examined. The activity of acrosomal enzymes was expressed as the fluorescence intensity (see *Materials and Methods*). Error bars indicate SEM data from three mice. Although the activity of acrosomal enzymes was mildly lower in *Prss37*−/− sperm, no significant differences were found.
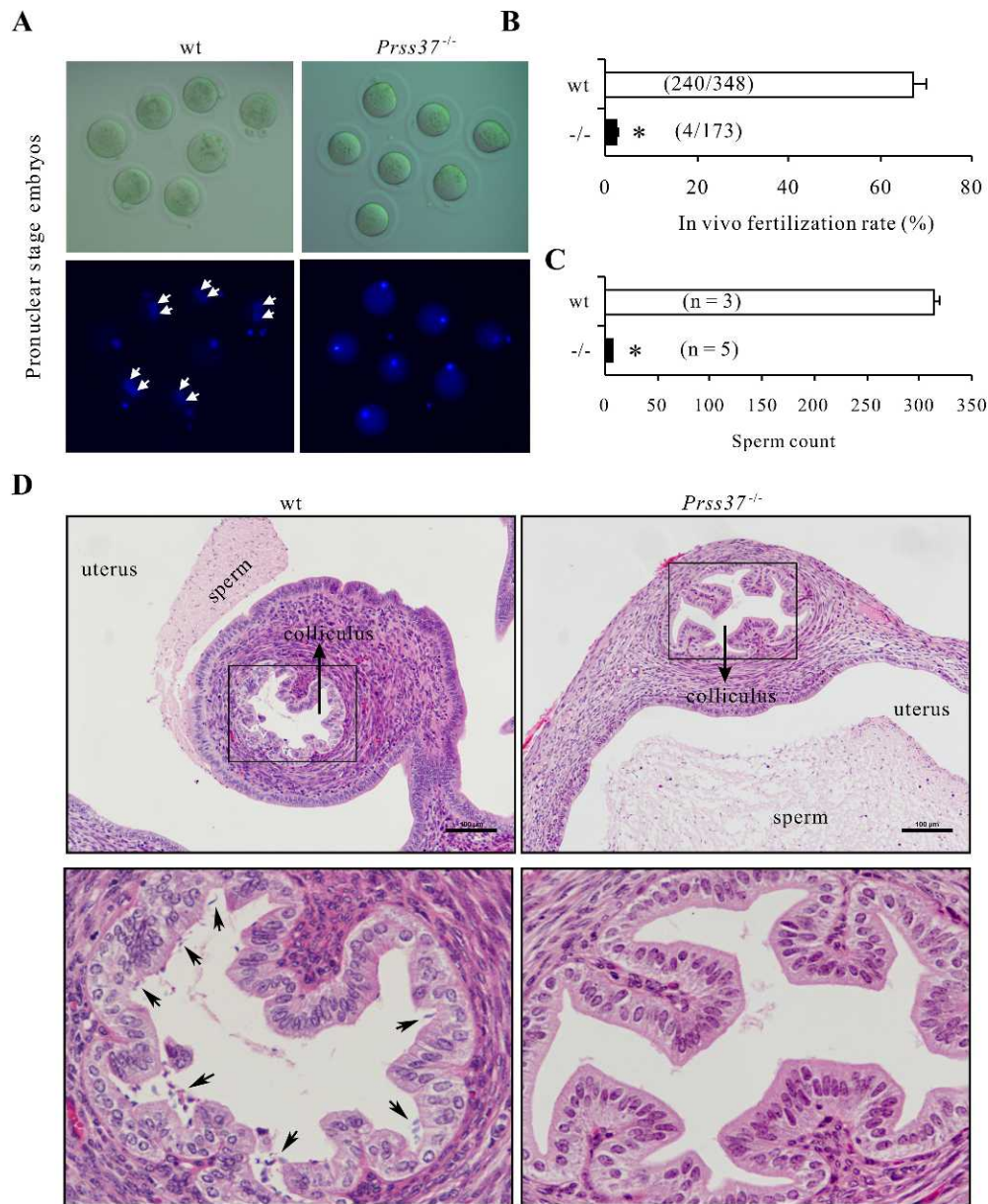
FIG. 5. Inability of *Prss37*$^{-/-}$ sperm to fertilize eggs in vivo. **A**) Pronuclear-stage embryos were observed by Hoechst 33258 staining. White arrows indicate the two pronuclei (2PN) formed inside the fertilized eggs. Brightfield images are shown in the top panels. **B**) In vivo fertilization rate was calculated as the ratio between the number of two-cell embryos recovered and the total number of two-cell embryos plus oocytes recovered. Data are means $\pm$ SEM from three separate assays, and the numbers in parentheses are the total two-cell embryos and two-cell embryos plus oocytes of three assays obtained. Asterisk indicates a significant difference ($P < 0.0001$) relative to the wt group, as determined by the unpaired Student *t*-test. **C**) Sperm number in the oviducts of plugged females 3.5 h after coitus with wt or *Prss37*$^{-/-}$ males were counted and analyzed. The number of plugged females examined in each genotype is shown in parentheses. Asterisk indicates a significant difference ($P < 0.0001$) relative to the wt group, as determined by the unpaired Student *t*-test. **D**) Defective migration of *Prss37*$^{-/-}$ sperm from uterus into oviducts. At 2 h after coitus, uteri and oviducts of plugged females mated with wt or *Prss37*$^{-/-}$ males were excised and fixed. Sections containing UTJ were made by serial sectioning and stained with H&E. Uterus, colliculus, and sperm ejaculated into uterus are shown in the top panels. Top panel insets show higher magnification. Arrows show sperm inside the colliculus. More than three plugged females mated with a male of each genotype were examined and representative images are shown. Bar = 100 µm.

Prss37$^{-/-}$ sperm was less than 10 (Fig. 5C). Migration defect of *Prss37*$^{-/-}$ sperm was also observed in sections containing UTJ 2 h after coitus. Few sperm from *Prss37*$^{-/-}$ mice were present in the colliculus (Fig. 5D, right panels), the initial part of the oviduct, while numerous sperm were observed in the nearby uterine lumen. On the other hand, when females were mated with wt males, sperm could be found in the colliculus (Fig. 5D, left panels). These findings suggest that defect in sperm migration from uterus into oviduct may occur in sperm from mutant mice.

Sperm from Prss37$^{-/-}$ Males Are Unable to Bind Zona-Intact Oocytes but Are Able to Fertilize Cumulus-Intact Oocytes In Vitro

We next characterized the function of *Prss37*$^{-/-}$ cauda epididymal sperm in vitro to address the question whether disruption of *Prss37* influences sperm–egg interaction and in vitro fertilizing ability. As shown in Figure 6A, incubation of *Prss37*$^{-/-}$ sperm with zona-intact eggs revealed the severely diminished ability of *Prss37*$^{-/-}$ sperm to bind to ZP (Fig. 6A,
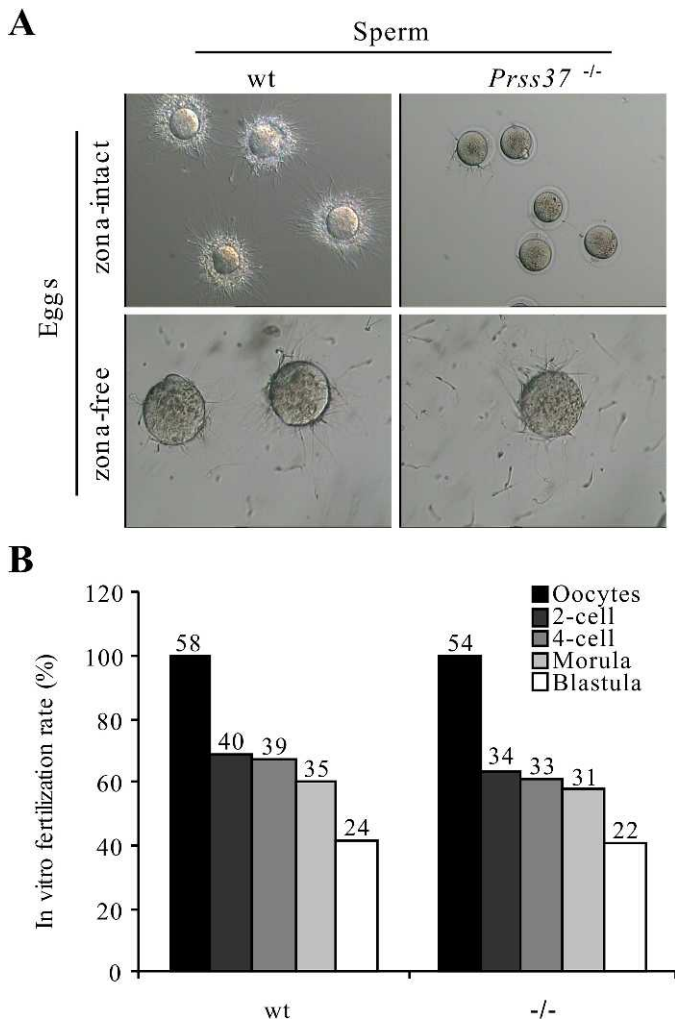
8

Article 123

FIG. 6. Sperm from *Prss37*^{−/−} males are unable to bind zona-intact oocytes but are able to fertilize cumulus-intact eggs in vitro. **A**) Zona-intact and zona-free eggs were incubated with cauda epididymal sperm capacitated in vitro. A large amount of wt sperm but only several or no *Prss37*^{−/−} sperm bound to zona-intact eggs (top panels). No significant differences were observed between wt and *Prss37*^{−/−} sperm in binding to zona-free eggs (bottom panels). This experiment was repeated more than three times, and images of a representative experiment are shown. **B**) Sperm from *Prss37*^{−/−} males were able to fertilize cumulus-intact oocytes in vitro, and the embryos were able to develop to blastula stage, comparable to those from wt males. The number of oocytes or embryos of different stages are shown in the graph. This experiment was repeated three times, and values are data from a representative experiment.
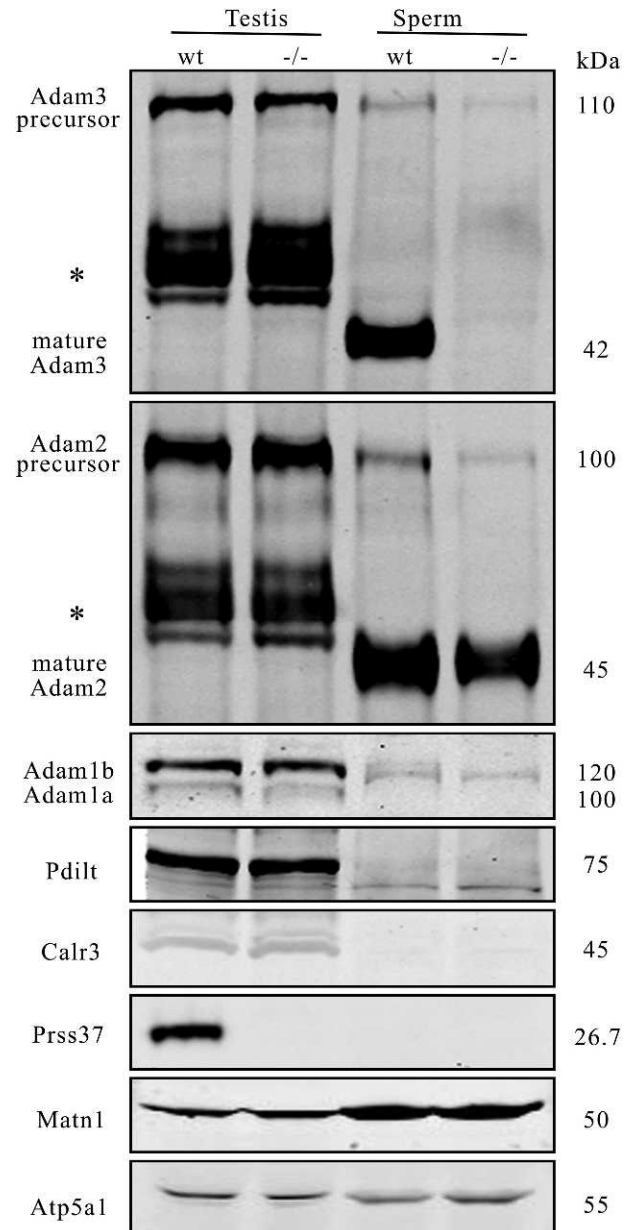

FIG. 7. *Prss37* deficiency affects the presence of mature Adam3 in sperm, with no significant impact on Adam1, Adam2, Pdilt, and Calr3. Both Adam3 and Adam2 antibodies recognized their respective precursor and mature forms. Asterisks indicate IgG signals recognized by the secondary antibodies. Adam1 antibody targeted the conserved region shared by Adam1a and 1b. Prss37 blot confirmed the genotypes of the samples. Blots of two other irrelevant sperm proteins (Matn1 and Atp5a1) are shown as loading controls. The sizes of specific protein bands are marked on the right.

top panels). However, there was no significant difference between wt and *Prss37*^{−/−} sperm in binding to zona-free eggs (Fig. 6A, bottom panels). These findings suggest that *Prss37* deficiency during spermiogenesis affects sperm-zona binding ability of sperm from *Prss37*^{−/−} males. Unexpectedly, sperm from *Prss37*^{−/−} males were capable of fertilizing cumulus-intact, ZP-intact oocytes normally, despite the impaired ability to bind the ZP (Fig. 6B). Moreover, a portion of these embryos were able to develop to blastula stage, with no significant differences between wt and *Prss37*-null groups. These observations were similar to those reported by other researchers [37–39], suggesting that sperm-zona binding ability might not be as important as we thought.

Mature Adam3 *Is Undetectable in Sperm from* Prss37^{−/−} *Males, but Its Precursor Remains Intact in Testis*

Considering the undetectable mRNA and protein levels of *Prss37* in epididymidis (Fig. 1, B and C), we presumed that Prss37 might not present in mature sperm or only at a very low level. Prss37 would be more likely to play an indirect role in sperm function. What are the target proteins affected by *Prss37* disruption?

Through a literature search, we found that nine other gene-disrupted mouse lines, including *Clgn* [40], *Ace* [41], *Adam2* [42], *Adam3* [43], *Adam1a* [37], *Calr3* [29], *Tpst2* [44], *Pdilt*

9

[38], and *Pmis2* [39], showed phenotypes with similar sperm migration defects and reduced sperm-zona binding abilities. Interestingly, all these mouse lines shared a common feature: Adam3 was absent or abnormally located in the mature sperm. Would Prss37 affect Adam3 presence or localization in sperm? To elucidate this possibility, we examined the presence of Adam3 in both testis and cauda epididymal sperm by Western blot analysis. As expected, the 42-kDa mature form of Adam3 was present in wt sperm but absent in *Prss37*$^{-/-}$ sperm, while the 110-kDa Adam3 precursor remained comparable between wt and *Prss37*$^{-/-}$ testes (Fig. 7). Previous reports have shown that disruption of *Adam2* and *Adam1a*, two other members of the Adam family, leads to defects in Adam3 maturation, and Calr3/Pdilt complex plays a role in regulating Adam3 folding and membrane transport [37, 38], deficiency of which results in the absence of mature Adam3 in sperm. However, it was found that Adam1a and Adam1b, capable of forming heterodimers with Adam2, respectively, remained unaffected in the testis lacking *Prss37*. Adam2 also showed comparable levels of precursor (100 kDa) in testis and mature form (45 kDa) in sperm between two genotypes. Furthermore, Pdilt and Calr3 were normally expressed in the testis deficient for *Prss37*. All these data suggest that *Prss37* deficiency causes the absence of mature Adam3 in sperm, which, however, is irrelevant to Adam1a, Adam2, Pdilt and Calr3 expressions.

DISCUSSION

Mammalian fertilization is a sequence of coordinated events involving multiple steps such as the sperm migration to destination, adhesion/binding and penetration of the ZP of oocytes, and fusion between sperm and oocytes. Various sperm factors have been reported to be important for successful fertilization in vivo, especially those verified by gene-targeting studies in mice [5, 45]. The ongoing efforts to identify the sperm-specific genes that are essential for fertilization are of great significance because they could contribute to explain male factor infertility in human and provide possible diagnosis and treatment approaches to achieve male reproductive health.

In the present study, we have demonstrated that Prss37, a previously uncharacterized putative trypsin-like serine protease, is crucial for male fertility. Male mice deficient for *Prss37* displayed normal sexuality, undisturbed testis development, normal sperm production, morphology, and in vitro motility but significantly impaired capability of sperm to fertilize eggs due to the defect in sperm migration from uterus into oviducts in vivo. Although the zona-binding ability of *Prss37*$^{-/-}$ sperm was severely impaired, it seemed irrelevant to the fertilizing ability of the sperm, as the in vitro fertilization (IVF) results suggested. The expression of Prss37 is strictly confined to the steps 9–14 of spermiogenesis. Considering the male infertility phenotypes resulted from *Prss37* deficiency together with its short expression time range, Prss37 could be a potential target for the development of male contraceptive drugs.

To understand the molecular mechanisms underlying the defects in sperm migration from uterus into oviduct and sperm-zona binding of sperm from *Prss37*$^{-/-}$ males, we discovered that mature Adam3 was completely vanished in the sperm, but its precursor remained unchanged in the testes of *Prss37*$^{-/-}$ males. Adam3 is an extensively investigated protein in literature. Up to now, at least eight other different gene-disrupted mouse lines except *Adam3*-null mice have been reported to influence the presence or localization of Adam3 in sperm [29, 37–42, 44]. Malfunction of Adam3 in these mutant mice unanimously causes male infertility. Our present work again provides a new infertile mouse model that relates to the

absence of mature Adam3 in sperm and its effects on sperm function. It is reasonable to consider that defects in sperm migration from uterus into oviduct and sperm-zona binding inability of sperm from *Prss37*$^{-/-}$ males are caused by the disappearance of mature Adam3 in sperm rather than the deficiency of Prss37 itself. Accordingly, the main cause of male infertility of *Prss37*-null mice is probably due to the lack of mature Adam3 in sperm rather than Prss37 deficiency. Adam3 is a sensitive downstream target of many testis and sperm proteins in mice, as reported by other researchers and our present work. The question is how Prss37 affects the presence of mature Adam3 in sperm. Linder et al. [32] previously located Adam3 in the acrosomal membranes of spermatids and spermatozoa, where Adam3 underwent post-translational modification during the epididymal transit. Coincidently, Prss37 was detected immunopositively in the acrosomal region of elongating spermatids dissected from testicular tubules by immunofluorescent microscopy (Supplemental Fig. S3). However, no direct interaction of Prss37 and Adam3 precursor could be detected, either in the testis or in cotransfected 293 cell line by co-immunoprecipitation assay (Supplemental Fig. S4). Supposing Prss37 functions as a serine protease, the absence of mature Adam3 in *Prss37*$^{-/-}$ sperm could be the result just of the loss of enzymatic activity. However, Prss37 protein was mainly expressed at steps 9–14 of spermiogenesis and disappeared before the appearance of mature Adam3 in sperm during the epididymal transit. Thus, Prss37 was unlikely to function as a protease that proteolytically cleaved Adam3 precursor. Taken together, Prss37 was more likely to affect the post-testicular proteolytic cleavage of Adam3 precursor through an intermediate(s). According to our data, we have excluded the affects of Adam1a, Adam2, Calr3 and Pdilt, so the intermediate factor(s) might be a novel protein. In spite of how these molecules affect the presence of mature Adam3 in mouse sperm, an essential role of mature Adam3 in the process of fertilization should not be neglected.

In summary, Prss37 is indispensible for male fertility in the mouse. Even though it is expressed in a short time range during spermiogenesis and does not exist in mature sperm, Prss37 indirectly affects the post translational modifications of Adam3 during epididymal transit. Sperm from *Prss37* deficient mice are absent of mature Adam3 and defective in migration from uterus into oviduct and sperm-zona binding, but still have normal fertilizing ability in IVF assays. The following issues need to be further investigated : 1) how Prss37 affects the presence of mature Adam3 in sperm; 2) how Prss37 and/or Adam3 affects sperm migration from uterus into oviducts; 3) how Prss37 and/or Adam3 affects sperm-zona binding; and 4) the relationship between the fertilizing ability and zona-binding ability of sperm.

REFERENCES

1. Andrade-Rocha FT. Semen analysis in laboratory practice: an overview of routine tests. J Clin Lab Anal 2003; 17:247–258.
2. Hamada A, Esteves SC, Agarwal A. Unexplained male infertility: potential causes and management. Human Andrology 2011; 1:2–16.
3. Abou-Haila A, Tulsiani DR. Mammalian sperm acrosome: formation, contents, and function. Arch Biochem Biophys 2000; 379:173–182.
4. Zheng H, Stratton CJ, Morozumi K, Jin J, Yanagimachi R, Yan W. Lack

of Spem1 causes aberrant cytoplasm removal, sperm deformation, and male infertility. Proc Natl Acad Sci U S A 2007; 104:6852–6857.

5. Matzuk MM, Lamb DJ. Genetic dissection of mammalian fertility pathways. Nat Cell Biol 2002; 4(suppl):s41–s49.

6. Kang-Decker N, Mantchev GT, Juneja SC, McNiven MA, van Deursen JM. Lack of acrosome formation in Hrb-deficient mice. Science 2001; 294:1531–1533.

7. Sapiro R, Kostetskii I, Olds-Clarke P, Gerton GL, Radice GL, Strauss IJ. Male infertility, impaired sperm motility, and hydrocephalus in mice deficient in sperm-associated antigen 6. Mol Cell Biol 2002; 22: 6298–6305.

8. Martianov I, Brancorsini S, Catena R, Gansmuller A, Kotaja N, Parvinen M, Sassone-Corsi P, Davidson I. Polar nuclear localization of H1T2, a histone H1 variant, required for spermatid elongation and DNA condensation during spermiogenesis. Proc Natl Acad Sci U S A 2005; 102:2808–2813.

9. Russell LD. Sertoli-germ cell interrelations: a review. Gamete Research 1980; 3:179–202.

10. Le Magueresse-Battistoni B. Serine proteases and serine protease inhibitors in testicular physiology: the plasminogen activation system. Reproduction 2007; 134:721–729.

11. Eisenbach M, Giojalas LC. Sperm guidance in mammals—an unpaved road to the egg. Nat Rev Mol Cell Biol 2006; 7:276–285.

12. Suarez SS, Pacey AA. Sperm transport in the female reproductive tract. Hum Reprod Update 2006; 12:23–37.

13. Page MJ, Di Cera E. Serine peptidases: classification, structure and function. Cell Mol Life Sci 2008; 65:1220–1236.

14. Hedstrom L. Serine protease mechanism and specificity. Chem Rev 2002; 102:4501–4524.

15. Gyamera-Acheampong C, Tantibhedhyangkul J, Weerachatyanukul W, Tadros H, Xu H, van de Loo JW, Pelletier RM, Tanphaichitr N, Mbikay M. Sperm from mice genetically deficient for the PCSK4 proteinase exhibit accelerated capacitation, precocious acrosome reaction, reduced binding to egg zona pellucida, and impaired fertilizing ability. Biol Reprod 2006; 74:666–673.

16. Gyamera-Acheampong C, Mbikay M. Proprotein convertase subtilisin/kexin type 4 in mammalian fertility: a review. Hum Reprod Update 2009; 15:237–247.

17. Kawano N, Kang W, Yamashita M, Koga Y, Yamazaki T, Hata T, Miyado K, Baba T. Mice lacking two sperm serine proteases, ACR and PRSS21, are subfertile, but the mutant sperm are infertile in vitro. Biol Reprod 2010; 83:359–369.

18. Baba T, Azuma S, Kashiwabara S, Toyoda Y. Sperm from mice carrying a targeted mutation of the acrosin gene can penetrate the oocyte zona pellucida and effect fertilization. J Biol Chem 1994; 269:31845–31849.

19. Yamagata K, Murayama K, Okabe M, Toshimori K, Nakanishi T, Kashiwabara S, Baba T. Acrosin accelerates the dispersal of sperm acrosomal proteins during acrosome reaction. J Biol Chem 1998; 273: 10470–10474.

20. Yamashita M, Honda A, Ogura A, Kashiwabara S, Fukami K, Baba T. Reduced fertility of mouse epididymal sperm lacking Prss21/Tesp5 is rescued by sperm exposure to uterine microenvironment. Genes Cells 2008; 13:1001–1013.

21. Zhang Y, Buchholz F, Muyrers JP, Stewart AF. A new logic for DNA engineering using recombination in Escherichia coli. Nat Genet 1998; 20: 123–128.

22. Liu P, Jenkins NA, Copeland NG. A highly efficient recombineering-based method for generating conditional knockout mutations. Genome Res 2003; 13:476–484.

23. Chen Q, Peng H, Lei L, Zhang Y, Kuang H, Cao Y, Shi QX, Ma T, Duan E. Aquaporin3 is a sperm water channel essential for postcopulatory sperm osmoadaptation and migration. Cell Res 2011; 21:922–933.

24. Quinn P, Kerin JF, Warnes GM. Improved pregnancy rate in human in vitro fertilization with the use of a medium based on the composition of human tubal fluid. Fertil Steril 1985; 44:493–498.

25. Mortimer D, Curtis EF, Miller RG. Specific labelling by peanut agglutinin of the outer acrosomal membrane of the human spermatozoon. J Reprod Fertil 1987; 81:127–135.

26. Zeginiadou T, Papadimas J, Mantalenakis S. Acrosome reaction: methods for detection and clinical significance. Andrologia 2000; 32:335–343.

27. Sutton KA, Jungnickel MK, Florman HM. A polycystin-1 controls postcopulatory reproductive selection in mice. Proc Natl Acad Sci U S A 2008; 105:8661–8666.

28. Ikawa M, Nakanishi T, Yamada S, Wada I, Kominami K, Tanaka H, Nozaki M, Nishimune Y, Okabe M. Calmegin is required for fertilin alpha/beta heterodimerization and sperm fertility. Dev Biol 2001; 240: 254–261.

29. Ikawa M, Tokuhiro K, Yamaguchi R, Benham AM, Tamura T, Wada I, Satouh Y, Inoue N, Okabe M. Calsperin is a testis-specific chaperone required for sperm fertility. J Biol Chem 2011; 286:5639–5646.

30. Erbach GT, Lawitts JA, Papaioannou VE, Biggers JD. Differential growth of the mouse preimplantation embryo in chemically defined media. Biol Reprod 1994; 50:1027–1033.

31. Zindy F, den Besten W, Chen B, Rehg JE, Latres E, Barbacid M, Pollard JW, Sherr CJ, Cohen PE, Roussel MF. Control of spermatogenesis in mice by the cyclin D-dependent kinase inhibitors p18(Ink4c) and p19(Ink4d). Mol Cell Biol 2001; 21:3244–3255.

32. Linder B, Bammer S, Heinlein UA. Delayed translation and posttranslational processing of cyritestin, an integral transmembrane protein of the mouse acrosome. Exp Cell Res 1995; 221:66–72.

33. Kleene KC. Poly(A) shortening accompanies the activation of translation of five mRNAs during spermiogenesis in the mouse. Development 1989; 106:367–373.

34. Ahmed EA, de Rooij DG. Staging of mouse seminiferous tubule cross-sections. Methods Mol Biol 2009; 558:263–277.

35. Bhattacharyya AK, Kanjilal S. Assessment of sperm functional competence and sperm-egg interaction. Mol Cell Biochem 2003; 253:255–261.

36. Honda A, Yamagata K, Sugiura S, Watanabe K, Baba T. A mouse serine protease TESP5 is selectively included into lipid rafts of sperm membrane presumably as a glycosylphosphatidylinositol-anchored protein. J Biol Chem 2002; 277:16976–16984.

37. Nishimura H, Kim E, Nakanishi T, Baba T. Possible function of the ADAM1a/ADAM2 Fertilin complex in the appearance of ADAM3 on the sperm surface. J Biol Chem 2004; 279:34957–34962.

38. Tokuhiro K, Ikawa M, Benham AM, Okabe M. Protein disulfide isomerase homolog PDILT is required for quality control of sperm membrane protein ADAM3 and male fertility. Proc Natl Acad Sci U S A 2012; 109:3850–3855.

39. Yamaguchi R, Fujihara Y, Ikawa M, Okabe M. Mice expressing aberrant sperm-specific protein PMIS2 produce normal-looking but fertilization-incompetent spermatozoa. Mol Biol Cell 2012; 23:2671–2679.

40. Ikawa M, Wada I, Kominami K, Watanabe D, Toshimori K, Nishimune Y, Okabe M. The putative chaperone calmegin is required for sperm fertility. Nature 1997; 387:607–611.

41. Hagaman JR, Moyer JS, Bachman ES, Sibony M, Magyar PL, Welch JE, Smithies O, Krege JH, O'Brien DA. Angiotensin-converting enzyme and male fertility. Proc Natl Acad Sci U S A 1998; 95:2552–2557.

42. Cho C, Bunch DO, Faure JE, Goulding EH, Eddy EM, Primakoff P, Myles DG. Fertilization defects in sperm from mice lacking fertilin beta. Science 1998; 281:1857–1859.

43. Shamsadin R, Adham IM, Nayernia K, Heinlein UA, Oberwinkler H, Engel W. Male mice deficient for germ-cell cyritestin are infertile. Biol Reprod 1999; 61:1445–1451.

44. Marcello MR, Jia W, Leary JA, Moore KL, Evans JP. Lack of tyrosylprotein sulfotransferase-2 activity results in altered sperm-egg interactions and loss of ADAM3 and ADAM6 in epididymal sperm. J Biol Chem 2011; 286:13060–13070.

45. Jamsai D, O'Bryan MK. Mouse models in male fertility research. Asian J Androl 2011; 13:139–151.